Taylor & Francis
Taylor & Francis Group

Dislocation processes that affect kinetics of fatigue crack growth

K. SADANANDA[†]* and G. GLINKA[‡]

[†]Code 6323, Material Science and Technology Division,
[‡]Naval Research Laboratory, Washington DC 20375, USA
Department of Mechanical Engineering, University of Waterloo,
Waterloo, Ontario N2L 3GI, Canada

Fatigue damage involves an irreversible plastic flow, and requires two load parameters for its unique description. We have examined the dislocation processes at the crack tip due to cyclic loads and showed that the two-parameter requirement naturally follows from the analysis. Hence, there are two fatigue thresholds, $K_{max,th}$ and ΔK_{th}, instead of just ΔK_{th}, as is normally assumed. Examination of dislocation behaviour reveals that the K_{max} threshold can be related to the stress necessary to nucleate additional slip needed for crack growth. Similarly, ΔK_{th} can be related to the stress to overcome reversible slip. The value of $K_{max,th}$ is always greater than or equal to ΔK_{th}. The two-parameter requirement can be related to the presence of monotonic and cyclic plastic zones characteristic of a fatigue crack. The size of monotonic plastic zone is always larger than that of the cyclic plastic zone. The former moves the crack tip forward while the latter re-sharpens it. The analysis also shows that the effect of crack wake plasticity on the crack tip driving force is limited and becomes increasingly negligible with increasing crack length. Dislocation concepts and continuum concepts are brought together to analyse the two-parameter requirement of fatigue crack growth.

1. Introduction

Fatigue is a plasticity-induced damage, and in crystalline materials it occurs by nucleation and motion of dislocations. Irreversibility associated with plastic flow governs the accumulation of the damage during cyclic loads. Cyclic loads require two load parameters to define them unambiguously: maximum or mean stress and stress amplitude. Goodman [1] more than a century ago established that both mean stress and stress amplitude affect fatigue life of a component subjected to cyclic loads. But for fatigue crack growth, only one driving force, the stress intensity factor range, ΔK, has been used for the quantification of crack growth rates [2]. The load ratio, R (R = minimum load/maximum load), is normally taken as the second parameter. However, unlike the mean stress in the Goodman diagram for fatigue life, the load ratio is not a driving force. Load ratio effects, therefore, have been

---

* Author for correspondence. Email: sada@anvil.nrl.navy.mil.

accounted for in fatigue crack growth analysis by bringing in an extrinsic factor called 'crack closure' [3].

Crack closure is the premature contact of crack surfaces that occurs at low R-ratios before the minimum load is reached. Such contact is assumed to reduce the applied stress intensity amplitude at the crack tip to an effective value. Plasticity in the wake of a growing crack is recognized as the major cause for the contact [3]. The explanation involves consideration of a zone of plasticity around the crack, which is further enclosed by an elastic material. The material in the plastic zone is considered as "stretched", while the rest of the material is elastically strained. When elastic unloading occurs, the plastic material is constrained and undergoes compression. Additional (over and above the elastic) crack-surface displacements due to these constraining forces are considered to be responsible for the premature contact. With larger unloading or decreasing minimum load, the contact effects will increase. Hence, at low R-ratios the crack closure effects predominate, reducing the applied ΔK to an effective amplitude ΔK_{eff}. Closure-free crack growth can only be obtained at high R-ratios ($R > 0.7$). Otherwise, a crack-closure correction is required to determine the effective stress intensity range ΔK_{eff}. Hence, in terms of ΔK_{eff}, there are no load-ratio effects, and there is only one load-parameter characterizing fatigue crack growth.

The experimentally measured values of crack closure, however, vary by more than 300% depending on the measurement location, technique employed [4–10], specimen geometry and crack length [11, 12], and environmental factors [13, 14]. We have shown that fatigue phenomena can be explained self-consistently using the fundamental concepts from dislocation theory, without invoking crack closure. In this paper we present the basis of our approach and its consistency with fracture mechanics concepts.

2. Dislocation concepts

We establish the following concepts based on dislocation theory:

(a) The crack-tip material undergoes shear rather than "stretch" during slip-induced plastic deformation. The plastic zone, by definition, involves a boundary between sheared and unsheared material, and therefore the presence of dislocations [15]. Distributed dislocations result due to the gradient in shear. Dislocations are internal-stress sources and a crack experiences the internal stresses from these dislocation fields. This implies that compressive stresses from plasticity do not arise only during unloading. They become operative as soon as dislocations are formed or when a plastic zone is formed. Under steady-state conditions, if the internal structure of a plastic zone is not altered significantly during each cycle, the internal stresses affect the crack-tip driving force during a complete cycle. That is, they affect K_{max} and K_{min}, while ΔK remains the same. In addition, these compressive forces operate whether crack-surface contact occurs or not, i.e. at all R-ratios.

(b) The resulting displacements of crack surfaces due to these stresses, the subsequent possibility of mating-surface contact, that in turn induces stresses that affect the crack tip driving force, is a circular argument. The stress field due to dislocations can directly affect the crack tip driving force.

Displacement-induced contact stresses could cause second-order effects, which should be considered if they are important. Experimental [16] and theoretical [17] analyses indicate that the effects of such contact stresses are negligible.

(c) Even the possibility of such crack–surface contact due to residual plasticity requires further examination. The analysis is simple. Plasticity at the crack tip opens up the crack. The monotonic plastic zone should be greater than the cyclic plastic zone. Therefore, the displacements in the forward direction should be more than displacements in the reverse direction. In addition, dislocation has to be a loop where a positive segment moves forward to form the plastic zone, while the negative segment is absorbed by a crack to form a ledge. The displacement due to positive dislocations can never be greater than the concentrated displacements due to ledges. This can also be stated in another way. Dislocation plasticity occurs at a constant volume. In forming a plastic zone, matter is removed from the crack and re-deposited in the plastic zone as dislocations. The displacements due to compressive stresses from these dislocations that are further away from the crack tip can never be greater than the displacements at the crack tip generated due to the removal of the matter.

(d) Finite element (FEM) analysis indicates that crack closure is observed not for a stationary crack but for a crack that moves into the plastic zone (movement is induced in the model by cutting the FEM nodes at the crack tip) [18]. It is interpreted as the needed plasticity in the crack wake to cause crack closure. However, under steady-state conditions, closure should occur even for a stationary crack during unloading. An alternative interpretation of the FEM result is that when the crack tip nodes are cut the crack is allowed to grow elastically (by cutting bonds) into the plastic zone where compressive stresses exist; and these compressive stresses ahead of the crack tip will now try to close the crack. Hence, it is the effect of internal stresses ahead of the crack tip that retards the growth rather than crack closure per se. The effect of these compressive stresses should be considered in calculating the stress necessary for the incremental plasticity, and should be considered in calculating the stresses necessary for the nucleation of new dislocations at the growing crack-tip. As has been noted, these stresses exist from the moment the plastic zone is formed and not necessarily only during unloading.

3. Two-threshold requirement

Consistent with Goodman's diagram [1] and the nature of the fatigue problem, we start with the assumption that fatigue involves two load parameters, each affecting the crack tip driving force. Correspondingly, there are two thresholds, one in terms of each parameter, which must be exceeded simultaneously for a fatigue crack to grow. Analysis of all the literature data of many metals, alloys, composites, and plastics indicates that the most appropriate parameters for crack growth are K_{max} and ΔK [19]. Thus, there exist two thresholds, $K_{max,th}$ and ΔK_{th}, that must be exceeded to have crack growth. Crack-growth data can be represented schematically in terms of these two parameters as shown in figure 1. Figure 1a shows a standard representation of fatigue threshold data in terms of R, while figure 1b shows a plot of
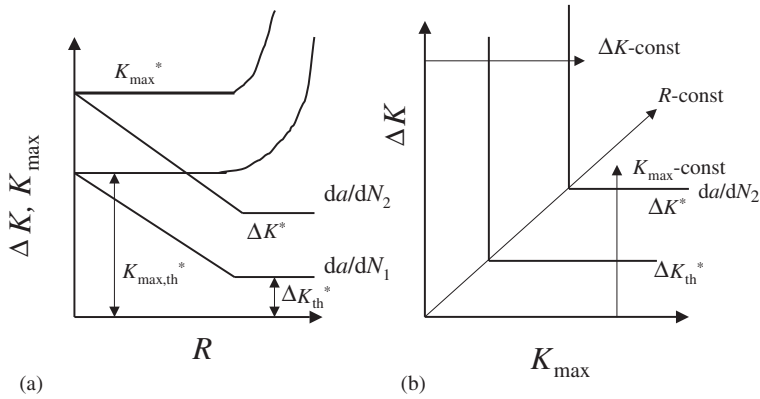
Figure 1.   (a) Conventional representation of ΔK and K_{max} at threshold as a function of load ratio, R. (b) ΔK–K_{max} plot for a given da/dN defining an L-shaped curve with two limiting thresholds and non-propagating regime.

ΔK vs. K_{max}. The data for almost all materials follow an L-shaped curve defining two thresholds and a non-propagating regime. It has been shown for almost all materials that $K_{max,th}$ is larger than ΔK_{th} and, hence, a more dominant parameter in controlling fatigue crack growth. Figure 2 shows typical experimental results for several low carbon steels [20]. In spite of variations in chemistry, microstructure, or processing conditions for various low carbon steels, ΔK_{th}^* remains the same while large changes in $K_{max,th}^*$ are noted. Similar results are observed in Al alloys [21].

4. Mechanisms governing the two fatigue thresholds

We examine at this stage the factors that determine the two fatigue thresholds by using the dislocation concepts. Understanding of the fundamentals of the fatigue crack growth process is still in the embryonic stage. The most familiar mechanisms in the literature are the plastic blunting process due to Laird [22] and alternate shear proposed by Neumann [23]. The first one gives an explanation of the formation of striations and the second provides the process in detail for a planar slip material. In both cases, the crack tip moves forward by dislocation generation at the crack tip. The crack growth increment in each cycle is related to the net Burgers vector that drives the crack tip forward. Cycle-by-cycle growth is ensured by incremental forward plasticity at the crack tip. An alternative mechanism is the cumulated damage process, wherein crack increment occurs intermittently by accumulated damage ahead of the crack tip. The details of these processes are again not clear. In either of the two mechanisms, the basic unit process is (a) forward slip involving the generation of a new dislocation for incremental plasticity, and (b) the reverse slip needed to re-sharpen the crack tip. In the language of mechanics, we can loosely relate these two requirements to monotonic plasticity and cyclic plasticity, respectively. These in turn can be related to the requirement of K_{max} and ΔK thresholds. On that basis, the two-parameter requirement and existence of two thresholds become intrinsic to fatigue. In this paper, we use this as the basis for determining the two thresholds.
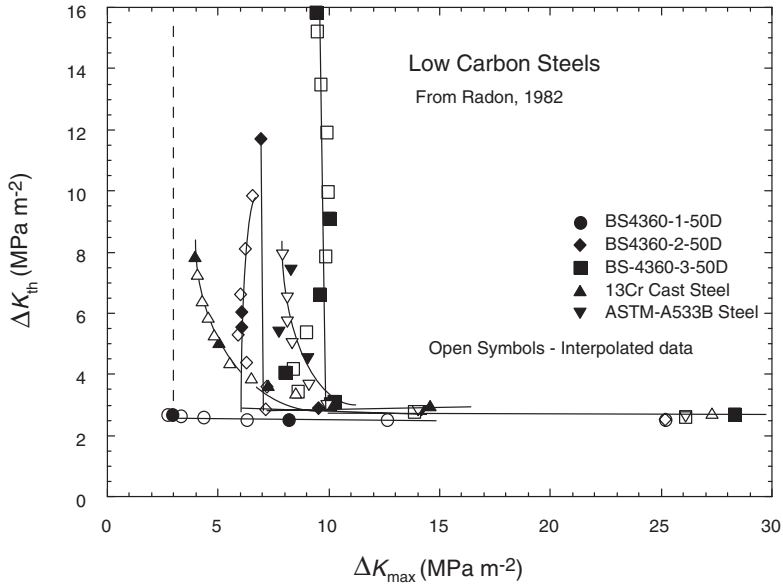
Figure 2. Experimental results for low-carbon steels showing large variation in $K_{\mathrm{max,th}}$ but not in ΔK_{th}.

5. Dislocation model for fatigue thresholds

5.1. *Dislocation process during loading*

A first dislocation model for fatigue crack growth threshold was developed earlier considering the stress necessary for dislocation generation [24] at the crack tip using Rice–Thomson's analysis [25]. We incorporate that analysis here considering now that the crack is surrounded by a steady-state plastic zone both at the crack tip and behind the crack tip.

Figure 3 provides a schematic description of sequence of dislocation process at the crack tip during loading and unloading. Figure 3a shows the loading and unloading during cycling, defining a peak load and an amplitude with load ratio $R = 0$. The stress intensity factor, K_{a}, at the crack tip provides a measure of the stresses at the crack tip due to a remote applied load, σ_{a}. Shear stresses are the maximum on a slip plane that is inclined around $70°$ to the crack plane. Figure 3b shows the first dislocation generation during loading when the shear stress on the slip plane near the crack tip exceeds the critical stress needed for dislocation generation and its glide. An associated ledge is formed and opens the crack. A detailed analysis of dislocation nucleation process at the crack tip has been given by Rice and Thomson [25]. Without losing the generality, we can approximately express the critical stress for dislocation generation [24] as

$$\sigma_{\mathrm{cr}} = \mu \mathbf{b}/(2\pi r) + \sigma_{\mathrm{f}} + \gamma_{\mathrm{s}} \tag{1}$$

where r is the critical distance for dislocation nucleation, μ is the shear modulus, $\mathbf{b}$ is the dislocation Burgers vector, σ_{f} is the lattice frictional force opposing dislocation motion, which is normally taken to be equal to the yield stress, and γ_{s} is the
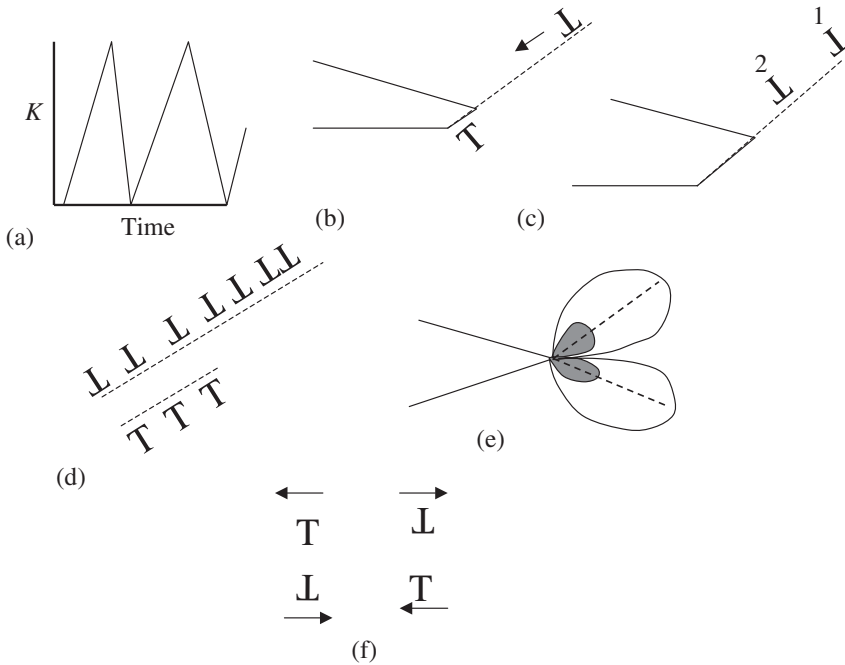
Figure 3. Schematic illustration showing the sequence of dislocation processes at the crack tip: (a) cyclic loads with peak load and amplitude, (b) nucleation of the first dislocation at the crack tip and the associated ledge, (c) nucleation of the second dislocation against the repulsive force from the first, (d) inverted dislocation pile-up formation and generation of dislocations of opposite sign forming dislocation dipoles, (e) formation of cyclic and monotonic plastic zones under steady-state conditions, and (f) passing stress needed to break a unit dipole which can control the threshold stress needed for to-and-fro dislocation motion.

surface energy in creating the ledge. The stresses due to crack tip must exceed this critical stress on the slip plane. Hence,

$$K_{\mathrm{a}} \geq \sigma_{\mathrm{cr}}\sqrt{(2\pi r)}/\Theta = K_{\mathrm{N1}}, \tag{2}$$

where

$$\Theta = \cos(\alpha/2)\sin(\alpha/2)\cos(3\alpha/2), \tag{3}$$

and where α is the angle of slip plane to the crack plane, and Θ is, thus, a measure of the trigonometric terms involved in the resolution of crack tip stresses on the slip plane, and K_{a} is the applied K_{max}. This critical K_{max} is designated as K_{N1}, i.e. the stress needed for nucleation of the first dislocation. After nucleation, this dislocation moves to a position where the force pushing the dislocation is balanced by the opposing friction. Frictional forces can increase with dislocation length as it gets jogged or cross slips during its glide. The nucleated dislocation now exerts opposing force on the crack tip, reducing the applied K at the crack tip by the term K_{D}, where K_{D} is the K due to the dislocation stress field. Lin and Thomson [26] have evaluated the K_{D} term for a semi-infinite crack. The stress needed for the nucleation of the second dislocation, figure 3c, is now $K_{\mathrm{N1}} + K_{\mathrm{D}}$ (algebraic sum is implied). Similarly, the third dislocation has to encounter the opposing forces from both the first and the second for its nucleation and glide. When the applied

stress reaches maximum load, a full monotonic plastic zone is formed and the size of the zone, r_y, can be given by continuum mechanics as [27]

$$r_y = \{K_{max}/\sigma_y\}^2/(\beta\pi) \qquad (4)$$

which is the same as the length of a dislocation-source pile-up emitted from the crack tip, (see figure 3d and 3e). Here β is 2 for plane stress and 6 for plane strain. The nth $+ 1$ dislocation that has to be nucleated has to overcome this critical stress for nucleation, which now includes, in addition to K_{N1}, the combined opposing forces from all the n dislocations that have been nucleated earlier. The combined opposing force from the dislocations in the monotonic plastic zone can be represented as K_{DT}, and the critical K for nucleation of nascent dislocation in the presence of a steady-state plastic zone is

$$K_{cr} = K_{N1} + K_{DT}. \qquad (5)$$

For simplicity, K_{DT} can be estimated by replacing the dislocation pile-up by a super-dislocation of equivalent strength [28]. From this it follows that the threshold for fatigue crack growth in terms of K_{max} is represented by equation (5) as

$$K_{max,th} = K_{cr}, \qquad (6)$$

and is related to the incremental plasticity needed for fatigue crack growth. Since close-form solutions for inclined edge-dislocation pile-up at the crack tip are not available, discrete dislocation models can be used to estimate K_{cr}. Discrete dislocation models will be analysed later.

5.2. *Dislocation processes during unloading*

The applied stress (K_a contribution) pushing all the dislocations forward decreases continuously with unloading. When the applied stress reaches zero, all the dislocations should, in principle, glide back into the crack tip. However the lattice frictional forces (treated as compressive yield stress in the continuum) oppose their reverse motion. Therefore, not all of the dislocations will glide back into the crack. This leaves residual plastic strain at the crack tip. This is the source of hysteresis energy.

The total reverse force on any dislocation i in the pile-up can be simply expressed as

$$\sigma_{ri} = \mu\mathbf{b}/(2\pi)\{\Sigma 1/(r_i - r_j)\} + \sigma_f - K_a(r), \qquad (7)$$

where summation is done with respect to all dislocations present on the slip plane with $j \neq i$. The dislocation force term is negative (compressive) from all the dislocations ahead of the ith dislocation (dislocations 1 to $i - 1$) and positive or tensile from all the dislocations behind (dislocations $i + 1$ to $n + 1$), as in figure 3d. Thus dislocation 1 has only tensile force while dislocation $n + 1$ has only compressive force due to all other dislocations in the plastic zone. (We are using terms "tensile" and "compressive" somewhat loosely, from the point of remote stress. The direction of the shear and dislocation movement changes correspondingly during loading vs. unloading).

Dislocations reverse back to the crack until the force on the dislocation falls below the resisting frictional force. The reverse movement of dislocations can also be thought of as forward movement of dislocations of opposite Burgers vector as shown

in figure 3d. The two opposite sets of dislocations essentially form dislocation dipoles near the crack tip. Thus near the crack tip we have a cyclic plastic zone, which differs from a monotonic plastic zone, where the dislocations are of one sign. A cyclic plastic zone is much smaller than monotonic plastic zone, as shown in figure 3e. The total amplitude necessary to overcome the lattice friction represents the minimum threshold ΔK_{th} required. For example, the Peierls–Nabarro force, which is a measure of lattice frictional force, can define the required amplitude. It is significantly small compared to the K_{max} required for crack growth. In reality, friction can also include all other processes that can resist a dislocation's to-and-fro motion, which include dislocation–dislocation intersections, formation of jogs, etc. In any case, threshold ΔK is much smaller than threshold K_{max}, as most of the experiments indicate. In addition, ΔK_{th} is less sensitive to most of the material variables. Many aluminium alloys, in spite of large variations in microstructure, essentially have the same fundamental ΔK threshold on the order of $1\,\text{MPa}\,\text{m}^{-2}$ [21]. The $K_{max,th}$ values, however, differ significantly among the alloys. These results imply that perhaps the intrinsic lattice resistance is the governing factor for the ΔK_{th}.

5.3. *Controlling parameter for fatigue crack growth*

Although there are two crack-tip driving forces and two critical values, one in terms of each, only one of the two will be the controlling parameter in a given range of R. For example, at high R-ratios, the K_{max} threshold requirement is easily met because of high mean stresses. In such cases, the fatigue will be governed by the ΔK threshold requirement. It is this threshold that experimentalists measure using high constant K_{max} tests (see figure 1). On the other hand, at low R-ratios (i.e when K_{min} is low and K_{max} is high), it is the K_{max} threshold that governs crack growth rather than the ΔK threshold, because of its relatively high magnitude. Thus the two-threshold stress requirement comes from the nature of the fatigue process; forward slip is required for crack growth and reverse slip is required to re-sharpen the crack.

5.4. *Dislocation dipole formation*

At high stresses, with the increase in dislocation density, the movement of dislocations can be governed by dipole formation and its break-up, as shown in figure 3f. The dipoles can be of interstitial or of vacancy type. Both types of dipoles have been observed under cyclic damage [29]. As the dislocation density increases, the spacing between the dipoles decreases and ultimately the fatigue damage is governed by the stress necessary to break up a unit dipole. The threshold ΔK can be related to the dipole strength, which is primarily a function of Burgers vector and dipole separation (height). Hence, ΔK_{th} is given by

$$\Delta K_{th} \approx A\mu\mathbf{B}/h, \tag{8}$$

where $\mathbf{B}$ is the Burgers vector of the dislocations involved in the dipole, and A is related to elastic constants discussed above. To evaluate the magnitude, we use a simple approximation based on the monotonic and reverse plastic zones as can be computed by continuum mechanics. Similarly the height, h, of the dipole should decrease with increase in crack growth rate (similar to the decrease of dislocation cell size with increased strain). As dipole separation h decreases, ΔK_{th} can be greater than the $K_{max,th}$. In that case, K_{max} has to equal ΔK. Under these conditions, a plot

of ΔK_{th} vs. K_{max} would give a 45° line. This relation, which is generally observed in the Paris regime, particularly in materials tested in vacuum, is called the pure fatigue line [30]. The crack growth in this case is governed by a reversibility condition, as dislocations have to move to-and-fro with dipole formation and its breakage.

6. Dislocation–crack interactions

Central to the evaluation of K_{max} threshold is the shielding effect of the dislocations in the plastic zone in the wake and at the crack tip. Recently James *et al.* [31] examined plasticity-induced crack closure using photoelasticity techniques but using material that can plastically deform near the crack tip. Based on their analysis, they concluded that there is no crack–surface contact during unloading, yet reduction in crack tip stresses occurs. They attributed this reduction to the shielding effect of plasticity at the crack tip and in the wake. Dislocations shield or anti-shield the crack-tip stress fields depending on their Burgers vector and position with respect to the crack tip. The K_{DT} term in equation (6) provides the effect of dislocation shielding on the crack tip stress intensity factor and is based on the Lin–Thomson [26] equations for a semi-infinite crack. In the following, we examine the shielding effect for a finite crack and compare the results with those of semi-infinite crack. We also show that these results can be deduced through the continuum approach by using weight function methods.

6.1. *Dislocation interactions with finite-size crack*

Zhang and Li [32] have analysed a finite crack with slip dislocations at both ends of the crack. The K_D term for a finite crack can be computed by considering a symmetrical configuration with pairs of dislocations at both ends (figure 4):

$$K_D = K_{DR} + K_{DL}, \tag{9}$$

where K_D is the total effect on any crack tip, K_{DR} is the contribution from the dislocations at the right edge, and K_{DL} is the contribution from the dislocations at the left edge. As the crack size increases, the results should converge to the semi-infinite case.

Figure 5 shows the K_D term as a function of the dislocation position in terms of y. The position of dislocation is ahead of the crack tip for $x/y > 0$ and in the wake of the crack for $x/y < 0$. The K_D term is also represented in non-dimensional form. The results for a semi-infinite crack are also represented in the plot. Here, α
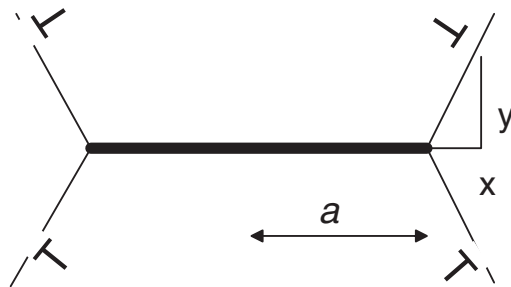

Figure 4. Finite crack with symmetrical distribution of dislocations at both ends.
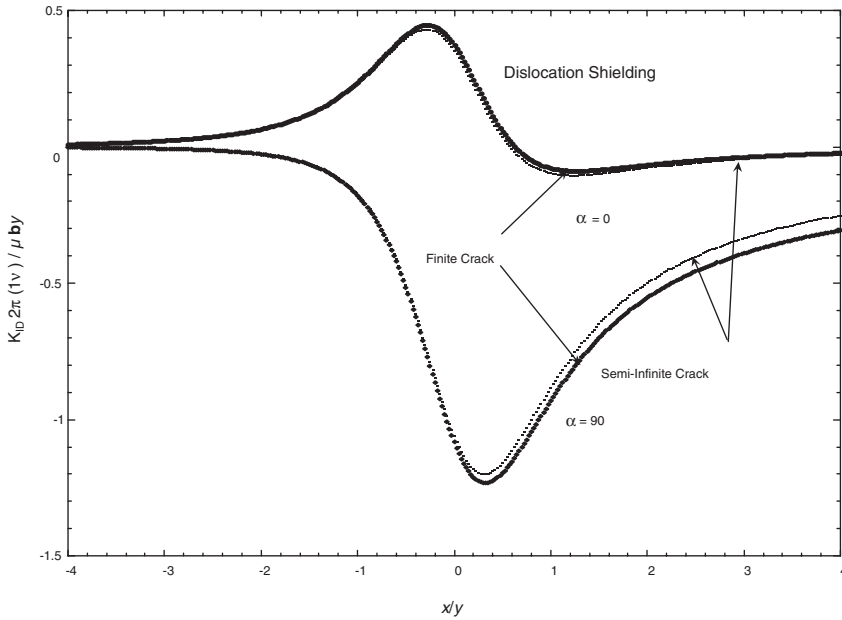
Figure 5. Variation of shielding effect of a dislocation as it moves towards the crack at constant y. Results for semi-infinite crack are also shown.

in the plot represents the Burgers vector orientation and is 0 for the x-component and $90°$ for the y-component.

Crack length is also expressed in units of y – but for purpose of calculations $2a/y$ is taken as 6. Figure 5 indicates that there is very little difference between the dislocation effects in finite and semi-infinite cracks. Hence, the results of a semi-infinite case are sufficiently accurate and consistent for purposes of our understanding. From the figure we can also conclude that the predominant shielding effect of dislocations or plasticity comes when the plastic zone is ahead of the crack tip. As the dislocation moves behind the crack tip, the effect dies down rapidly, and for $x/y < -2$ the effect is almost zero. In the case of $\alpha = 0$ the effect becomes anti-shielding, inducing a slightly positive force on the crack tip. Hence, any crack retarding force from the crack wake plasticity should be negligible. This result can be seen intuitively to be true. As the dislocation moves behind the crack tip, the distance between dislocation and the crack surface (or essentially the width of the plastic zone in the wake) becomes smaller in comparison to the crack length. Hence, the image effects due to the close proximity of the free crack-surface reduce any long-range effects of the plastic wake. The implication is that for distances greater than twice the width of the plastic wake, its effect on the crack tip-driving force is essentially zero. This has important bearing on the role of crack tip plasticity in the wake of a crack tip.

6.2. *Continuum analysis*

Glinka [33] has used weight function methods [34] to evaluate the stress intensity factor arising from dislocation stress fields. For a crack of a finite size, using the elastic stress field of dislocations [35], the effect on the crack tip driving force, K_D,
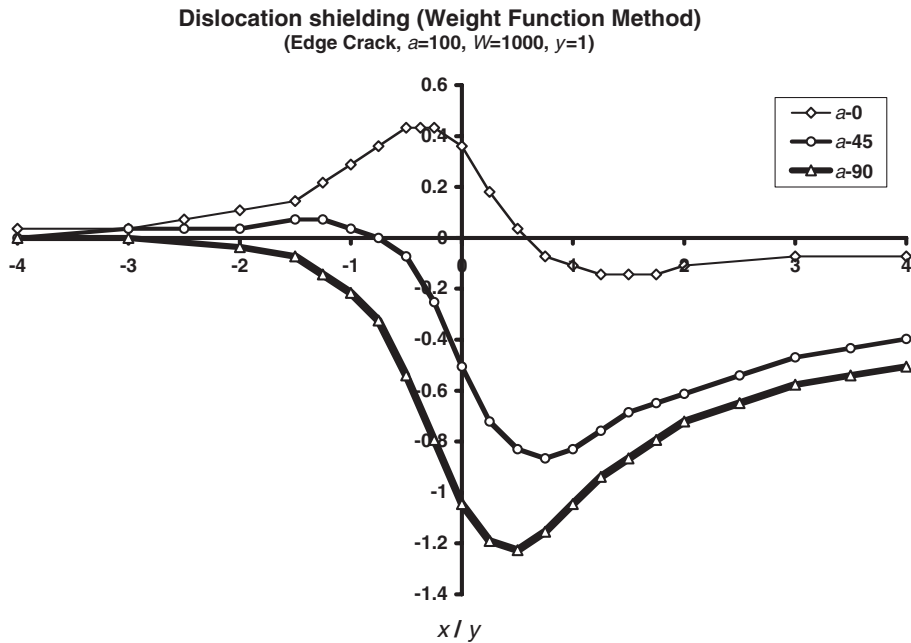
Dislocation shielding (Weight Function Method)
(Edge Crack, *a*=100, *W*=1000, *y*=1)

Figure 6. The effect of dislocation stress field on the crack tip stress intensity factor K deduced using the weight function method.

was computed as a function of dislocation separation from the crack tip. In his calculations, Glinka [33] froze the dislocations' position but moved the crack by expanding its size. In contrast, in figure 5, the crack size is fixed while the dislocation is moved to form crack-wake plasticity. The results are shown in figure 6. Comparison of figures 5 and 6 shows that whether the crack moves forward or the plastic zone moves behind the crack tip the effects are similar, and it reconfirms the earlier result that size of the crack has less effect since, in figure 6, crack size is altered as it grows. All the results are self-consistent and we conclude, therefore, that the shielding effect from dislocation plasticity arises mostly from the plasticity close to the crack tip. The dislocation stress fields act as internal stresses, which retard the crack-tip force. This force has to be exceeded for a crack to move forward. Since it is not of cyclic nature, it controls the K_{max} requirement. The monotonic plastic zone itself provides the basic factor opposing the crack movement; hence it defines the K_{max} threshold required for fatigue crack growth. This is, however, only a necessary condition but not a sufficient condition. Environment, for example, can alter the surface energy term and thus affect nucleation. In addition, it can induce embrittlement mechanisms that affect the K_{max} value. Figure 6 demonstrates that continuum and discrete dislocation analysis can be combined to arrive at self-consistent results.

6.3. *Discrete dislocation analysis*

The analysis thus far has considered crack–tip plasticity in terms of a superdislocation with dislocation strength equal to half of the CTOD. In the following, we analyse the problem in terms of a discrete dislocation model. For simplicity,
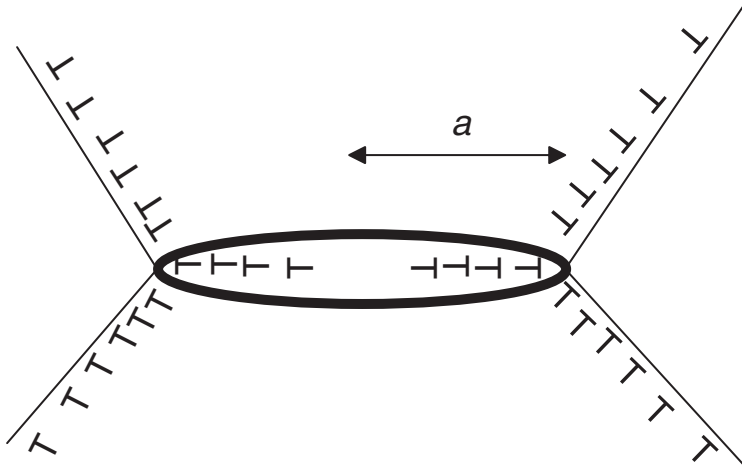
Figure 7. Discrete dislocation model of a crack with crack and crystal lattice dislocations present.

we replace the crack with discrete dislocations of varying Burgers vector (crack dislocations) [36, 37] and plasticity with dislocations with finite Burgers vector (crystal lattice dislocations) on a $70°$ inclined slip plane as shown in figure 7. To arrive at an equilibrium configuration of the system under remote stress, we minimize the total energy of the system, which can be written as

$$E_{\mathrm{T}} = E_{\mathrm{s}} + E_{\mathrm{I}} + E_{\gamma} + E_{\sigma\mathrm{a}} + E_{\sigma\mathrm{f}} \tag{10}$$

where E_{s} is the self-energy of all the dislocations, E_{I} the mutual interaction energy of all the dislocations, E_{γ} the surface energy, $E_{\sigma\mathrm{a}}$ the work done by applied stress and $E_{\sigma\mathrm{f}}$ the work expended against frictional forces. Expressions for each can be obtained from any standard dislocation theory book [35]. The self-energy of the dislocations involves summation of energy of all dislocations (crack + crystal lattice). Similarly, the interaction energy term includes interaction of crack–crack dislocations, crack–crystal lattice dislocations, and crystal lattice–crystal lattice dislocations taking into consideration that a dislocation does not interact with itself. The surface energy term includes the crack surface energy as well as the energy of the ledge as the crystal lattice dislocations emerge from the crack tip. The work done by the remote applied stress is sum of work done to move the crack dislocation inside the crack and work done by the resolved shear stress to move crystal lattice dislocations on their plane. The lattice frictional energy comes into play only for crystal lattice dislocation, where we use crack tip as the reference for the computation of the energy. Since friction is a non-conservative force, care is taken to ensure that the dislocations move in sequence in one direction only during loading. In the calculations, the crack is filled with crack dislocations until no more can be packed while minimizing total energy with respect to positional coordinates. As the Burgers vector of crack dislocations is reduced, the number density required to pack the crack increases. In the limit of infinitesimal Burgers vectors, the equilibrium (energy minimum) corresponds to the traction-free stress state of crack surfaces. For computational expediency, a variable Burgers vector for crack dislocations is used, with the largest Burgers vector for the dislocation at the crack tip.

In the present analysis, we initially fix the size of a crack and let it relax by pumping dislocations on the glide plane, using reasonable values for applied and frictional stresses. For the elastic modulus and surface energy, typical values corresponding to, say, Fe are used. The results, however, are sufficiently general and are not restricted to the specific values selected. The purpose of this exercise is to evaluate the degree of approximation involved in replacing the plastic zone by a super-dislocation model. For this purpose, after determining the equilibrium configuration with the dislocations originating from the crack tip, the crystal lattice dislocations are locked-in and the crack is moved forward elastically. For each increment in crack size, the new equilibrium configuration of all dislocations (crack + crystal lattice) is determined by minimizing the total energy, equation (15). For each new calculation, old equilibrium positions of the crystal lattice dislocations are taken as reference. This implies that if the dislocations move back towards the crack, they have to expend the energy against friction. Friction, in fact, prevents the complete collapse of the dislocations due to backward motion. For each crack size increment, the crack has to be repacked with crack dislocations until it is again full. Calculations in a sense simulate realistic changes that occur in the plastic zone as it moves to form crack-wake plasticity. In addition, the energy minimization ensures that crack surfaces are traction-free all the time, and, hence, includes all the dislocation-image forces in the formulation.

Once the dislocation configuration on the inclined slip plane is determined, the K_D (normalized value) of each dislocation in the plastic zone is calculated using equations deduced by Lin and Thomson [26]. The results are shown in figure 8. In presenting the results we have normalized the ordinate with a y-value corresponding to the 1/4 of the plastic zone size. It represents approximately the "centre of gravity" of dislocations in a pile-up. In the discrete dislocation model, the plastic zone originates from the crack tip. Hence x/y at the starting point of the calculations is
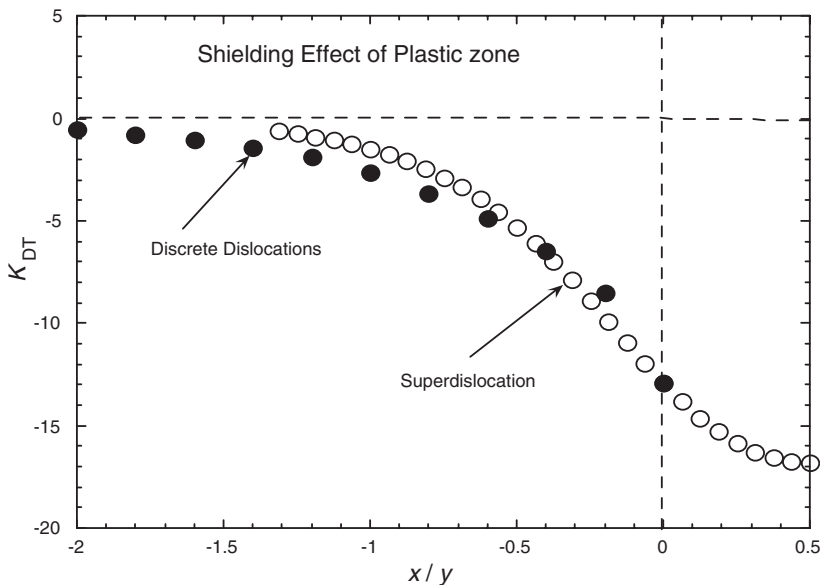

Figure 8. Comparison of the results of discrete dislocation calculations with those of super-dislocation model.

zero. For a superdislocation of equivalent net Burgers vector, the calculations can be done for any x/y value. Figure 8 shows that results are surprisingly close, indicating that superdislocation analogue is not far from reality. The effect is predominant when the dislocations are ahead of the crack tip. Larger negative values for discrete dislocations are expected for $x/y < 0$ since some of the dislocations close to the end of the plastic zone may still be ahead of the crack tip contributing to a larger share of the shielding effect. The fact remains that the shielding effect rapidly goes to zero as the plasticity moves behind by more than twice its width.

Here we have not considered the unloading process and how the dislocation configuration changes. It is assumed that frictional forces will hold the dislocations thus generated. In the fracture mechanics analysis using FEM, it is generally assumed that compressive yield stress opposes the reverse plasticity. However, the crack dislocations will collapse during unloading and one may have to fill the crack with anti-crack dislocations [37] in order to keep the crack surfaces traction-free. The concept is somewhat similar to notches under compression. This can be done if one assumes that the crack remains open like a notch. That, however, presupposes the results in the evaluation of crack closure. More appropriate calculations would examine the behaviour of a continuously growing crack with continuous evolution of the plastic zone both ahead and behind the crack tip. These calculations are currently underway and will be reported later.

7. Summary and conclusion

We have examined the dislocation behaviour at the growing fatigue crack. Under steady state conditions, the monotonic plastic zone formed exerts compressive stresses at the crack tip and retards its growth. For crack growth to occur, the stress should exceed the stress to nucleate new dislocations against this retarding force. Hence the threshold K_{max} required for crack growth can be related to the stress necessary for this incremental plasticity. We have analysed the problem by replacing the plastic zone by a superdislocation of equivalent Burgers vector, using both semi-infinite and finite cracks. In addition, we have shown that the results agree closely with the discrete dislocation analysis. The second threshold requirement, ΔK_{th}, is related to the reversible slip needed to re-sharpen the crack tip. At high strains, the two thresholds can be become equal to the stress necessary to break a dislocation dipole. It is shown from dislocation considerations that crack closure is not necessary to account for the fatigue crack growth behaviour. The fatigue crack growth analysis reduces to a basic fracture mechanics problem preserving the law of similitude without any need of extrinsic factors.

Acknowledgements

References

[1] J. Goodman, *Mechanics Applied to Engineering* (Longmans Green, London, 1899).

[2] P.C. Paris, M.P. Gomez and W.E. Anderson, Trends Engng **13** 1452 (1961).
[3] W. Elber, Engng Fract. Mech. **2** 37 (1970).
[4] D.E. Macha, D.M. Corby and J.W. Jones, Proc. Soc. Exp. Stress Analysis **36** 207 (1979).
[5] C.S. Shin and R.A. Smith, Int. J. Fatigue **7** 87 (1985).
[6] ASTM Round Robin Tests, in *Mechanics of Fatigue Crack Closure*, ASTM Special Technical Publications **982** 139 (1988).
[7] J.K. Donald, Int. J. Fatigue **19** 191 (1997).
[8] J.K. Donald, G.H. Bray and R.W. Bush, paper presented at 29th National Symposium on Fatigue and Fracture Mechanics (1998).
[9] P.C. Paris, H. Tada and J.K. Donald, Int. J. Fatigue **21** S35 (1999).
[10] D. Kujawski, Int. J. Fatigue **23** 95 (2001).
[11] B.L. Josefson, T. Svensson, J.W. Ringsberg and T. Gustafsson, J. deMare, Engng Fract. Mech. **66** 223 (2000).
[12] L.W. Wei and M.N. James, Engng Fract. Mech. **66** 587 (2000).
[13] B.R. Kirby and C.J. Beevers, Fract. Engng Mater. Struct. **1** 303 (1979).
[14] J.E. King, Fract. Engng Mater. Struct. **5** 177 (1982).
[15] V. Volterra, Ann. Ecole norm. super. **24** 400 (1907).
[16] R.W. Hertzberg, C.H. Newton, R. Jaccard, in *Mechanics of Fatigue Crack Closure*, ASTM Special Technical Publications **982** 139 (1988).
[17] N. Louat, K. Sadananda, M.S. Duesberry and A.K. Vasudevan, Metall. Mater. Trans. A **24** 2225 (1993).
[18] J.C. Newman, Jr., Int. J. Fract. **24** R131 (1984).
[19] A.K. Vasudevan and K. Sadananda, Metall. Trans. A **26** 1221 (1995).
[20] J.C. Radon, *Fatigue Thresholds* vol 1 (EMAS Publications, Warley, West Midlands, UK, 1982), p. 113.
[21] A.K. Vasudevan and K. Sadananda, Scripta metall. **28** 837 (1993).
[22] C. Laird, in *Fatigue Crack Propagation*, ASTM Special Technical Publications **415** 131 (1967).
[23] P. Neumann, Acta metall. **17** 1219 (1969).
[24] K. Sadananda and P. Shahinian, Int. J. Fract. **13** 585 (1977).
[25] J. R. Rice and R. Thomson, Phil. Mag. **29** 73 (1974).
[26] I.-H. Lin and R. Thomson, Acta metall. **34** 187 (1986).
[27] J.R. Rice, *Treatise on Fracture* (Academic Press, New York, 1967).
[28] K. Sadananda and D.N. Ramaswamy, Phil. Mag. **81** 1283 (2001).
[29] C. Laird, *Fatigue and Microstructure* (American Society for Metals, Metals Park, OH, 1979) p.149.
[30] K. Sadananda, A.K. Vasudevan and R.L. Holtz, Int. J. Fatigue **23** S277 (2001).
[31] M.N. James, M.N. Pacy, L.W. Wei and E.A. Patterson, Engng Fract. Mech. **70** 2473 (2003).
[32] T.-Y. Zhang and J.C.M. Li, Acta metall. mater. **39** 2739 (1991).
[33] G. Glinka, *Analytical and Numerical Evaluation of the Crack Tip Closure Effect on Fatigue Crack Growth* (University of Waterloo, Canada, 2002).
[34] G. Shen and G. Glinka, Engng. Fract. Mech. **40** 1135 (1991).
[35] J.P. Hirth and J. Lothe, *Theory of Dislocations* (McGraw Hill, New York, 1968)
[36] K. Sadananda, K. Jagannadham and M.J. Marcinkowski, Phys. Stat. Sol. (a) **44** 633 (1977).
[37] K. Jagannadham and M.J. Marcinkowski, *Unified Theory of Fracture* (Trans Tech. Publications, Aedermannsdorf, Switzerland, 1983).